

Predictive, distributed, hierarchical charging control of PHEVs in the distribution system of a large urban area incorporating a multi agent transportation simulation

Matthias D. Galus, R. A. Waraich, Göran Andersson

ETH Zurich

Zurich, Switzerland

galus@eeh.ee.ethz.ch, andersson@eeh.ee.ethz.ch

Abstract - The paper describes a method for investigating the impacts of wide-scale Plug-In Hybrid Electric Vehicle (PHEV) integration in electricity networks. It incorporates an agent-based transportation micro-simulation, which provides detailed temporal and spatial information of PHEV behavior including vehicle connection times, locations and energy demands. These inputs are subsequently used in power systems simulations. The power system model incorporates smart management devices which distribute, potentially scarce, power efficiently between connected PHEVs. These management devices ensure a secure power system operation. The integrated transportation and power system model provides detailed insights on impacts of wide scale PHEV adoption on electricity systems, outlines expansion needs and provides a proof of concept for the operability of a future smart grid.

Keywords - *Plug-In Hybrid Electric Vehicles (PHEVs), agent based modeling, transportation simulation (MATSim), distribution system analysis*

1 INTRODUCTION

Plug-In Hybrid Electric Vehicles (PHEVs) and electric vehicles offer the potential to increase efficiency in the individual transportation sector by replacing a substantial fraction of gasoline by electricity. Currently, the temporal and spatial distribution of the PHEVs is hard to anticipate which causes challenges when assessing and planning future grid expansion and grid operation [1]. The recharging behavior currently assumed in literature is based either on household surveys [2] or based on demographics [3].

It has been shown that wide scale PHEV utilization can cause asset overloading and voltage instabilities if recharging is performed in an uncontrolled manner. Controlled recharging can avoid endangering network security. However, such smart charging schemes have so far only been illustrated for small networks and complete information on vehicle behavior. Vehicle behavior is modeled on rough assumptions which include the spatial and temporal behavior as well as energy demands, i.e. battery energy levels, at arrival and departure [2, 4].

This paper contributes on several levels to the assessment of electric mobility. In contrast to other publications, the temporal and spatial vehicle behavior is simulated by an agent based transportation simulation tool. It includes realistic vehicle energy consumption profiles which are derived from the vehicle model elaborated in [5]. Furthermore, the paper shows how a controlled recharging scheme, based on the transportation simulation output, can be integrated into the electricity network of the city of

Zurich, Switzerland, thereby transforming it into an intelligent power system. The wide scale distributed deployment of hierarchical control devices [6], which manage PHEV demand, ensures network security by avoiding the overloading of assets, such as transformers, and by averting deep voltage sags. The management scheme could be used by a distribution network operator or a PHEV aggregator whose services are called upon by the network operator. The scheme presented herein demonstrates the operability of a future smart grid.

The paper is structured as follows. In Section 2 the agent based transportation model, which is used to simulate the PHEV behavior, is described. Section 3 introduces the power system of Zurich and Section 4 outlines PHEV management scheme, organized in a distributed, hierarchical structure. In Section 5 case studies show the operability of a smart grid, incorporating the PHEV demand management and ensuring system security. Section 6 summarizes the results and provides conclusions.

2 AGENT BASED TRANSPORTATION SIMULATION

The transportation behavior of the population can be modeled and simulated through agent-based approaches, one of which is a tool referred to as Multi Agent Transportation Simulation (MATSim) [7]. MATSim is a micro-simulation in which every individual which travels through the system is modelled by an agent k , where

$$k \in \mathcal{K} = \{1, 2, \dots, K\} \quad (1)$$

and \mathcal{K} is the set of all agents.

The advantage of modeling every individual participant in the transportation environment is the detailed insights into the spatial and temporal distribution of the agents which are obtained from the output. The output includes the agents' battery state at arrival and departure, where the latter is given by the model constraint that the vehicles should always be recharged to a level which allows them to reach their next destination. The transportation model gives detailed information on traffic, on, in general, behavioral patterns and in particular their evolution, when the agents' environment is adapted to the real world; including activities such as "work", "home", "shop", "leisure", etc.

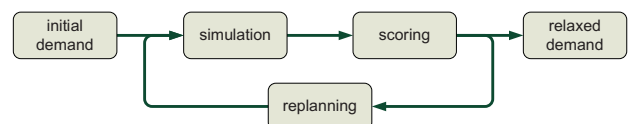


Figure 1: Co-evolutionary simulation process of MATSim

MATSim is based on the co-evolutionary algorithm depicted in Fig. 1. First, an initial demand of the agents is created. This demand incorporates the agents' daily demand for activities given by the activity durations, the start and end times as well as their respective locations. The activities a of agent k are denoted

$$a \in \mathcal{A}_k = \{1, 2, \dots, N_k^A\} \quad , \quad (2)$$

where \mathcal{A}_k is a list of activities ordered by their time of execution. The location of agent k 's activity a is expressed as

$$loc_{k,a} = \{x_{k,a}, y_{k,a}\} \quad , \quad (3)$$

where $x_{k,a}$, $y_{k,a}$ are the cartesian coordinates of the activity expressed in Geographical Information System (GIS) coordinates. All locations of the MATSim environment are contained in the set

$$\mathcal{LOC} = \{loc_{k,a}\} \forall k \in \mathcal{K} \wedge \forall a \in \mathcal{A}_k \quad . \quad (4)$$

The daily plans are executed in MATSim which results in computed starting and ending times of agent k 's activities. These results can differ from the agent's initial plan due to environmental factors, such as road congestion. The result is scored.

The scoring functions allocate gains/costs to the agents based on the duration for which the activity was performed, on the time spent in traffic, for late or early arrival at an activity, and for running low on energy, etc. After scoring, a replanning is performed. This step uses a genetic algorithm to generate new plans and routes for the agents [8]. Then, the execution of the plans is performed again. This update is repeated until the agents' behavior is no longer altered. This state is called a transportation equilibrium [9]. It is taken as an input for the power system simulation which considers the electricity demand of the PHEVs. The obtained results are valid under the assumption that transportation behavior is not altered. When departing from an activity and having failed to achieve the desired state of charge (SOC) at departure, it is assumed that the agent does not change its transport and recharging behavior.

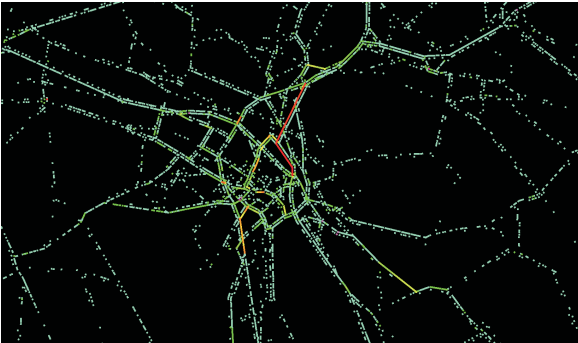


Figure 2: This figure visualizes the location and speed of all agents in the middle of the city of Zurich, at around 6:30 in the morning. Agents colored red have a low speed and compared to the free speed of the road and are stuck in a traffic jam. Source: www.matsim.org

Fig. 2 illustrates a typical temporal snapshot of the MATSim output for the city of Zurich, incorporating ca. 26'000 streets. The dots depict the individual agents on the streets. Red colored dots depict agents limited by traffic jams. Green dots indicate agents which can move through the streets freely.

3 THE ELECTRICITY SYSTEM OF ZURICH

The electricity grid of the municipality of Zurich comprises several voltage levels including a 380 kV network, the 150 kV network intra urban high voltage network and the 11/22 kV intra urban distribution network. Lower voltage levels are not considered here. The nodes at the 11/22 kV level are referred to as

$$n \in \mathcal{N} = \{1, 2, \dots, N\} \quad , \quad (5)$$

where

$$loc_n = \{x_n, y_n\} \quad , \quad (6)$$

gives the GIS coordinates of the electric node n . The nodes on the 11/22kV-level incorporate transformers which are rated so that they are loaded to 60% at maximum load hours.

For the purpose of integrating transportation and power system simulations, GIS coordinates of activity locations $loc_{k,a}$, i.e. street coordinates, are clustered according to their proximity to the network nodes. This means that coordinates of several activity locations are assigned to the node which models the load for the particular activity area. The mapping is expressed as a function

$$f_1 : \mathcal{LOC} \rightarrow \mathcal{N} \quad , \quad (7)$$

with

$$f_1(\mathcal{LOC}) := \{n \in \mathcal{N} | \exists loc_{k,a} \in \mathcal{LOC} : f_1(loc_{k,a}) = n\} \quad (8)$$

PHEVs, which are connected during time period T at node n , are denoted as

$$v \in \mathcal{V}_n(T) = \{1, 2, \dots, N_n^{\text{PHEV}}(T)\} \forall n \in \mathcal{N} \quad , \quad (9)$$

where

$$\mathcal{V}_n(T) \subseteq \mathcal{K} \quad . \quad (10)$$

Nodes at the 11/22kV level are clustered in zones and fed from transformers installed at the 150 kV level. Each 150 kV transformer feeds a single zone. The zones are not connected to each other and are subsequently denoted

$$z \in \mathcal{Z} = \{1, 2, \dots, Z\} \quad , \quad (11)$$

where each zone is made up of nodes

$$n_z \in \mathcal{N}_z = \{1, 2, \dots, N_z\} \quad , \quad (12)$$

and

$$\mathcal{N}_z \subseteq \mathcal{N} \quad . \quad (13)$$

The described power system used for the simulations is depicted in Fig. 3 and the number of elements defining the system is given in Tab. 1.

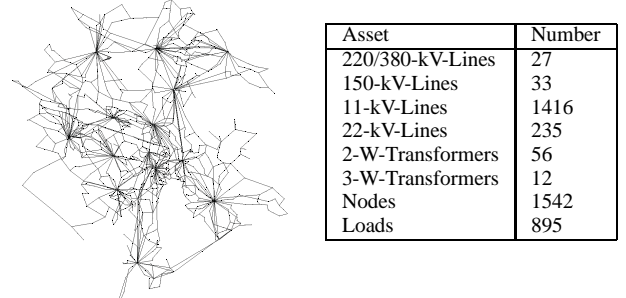


Figure 3: Electricity distribution network of Zurich, Switzerland **Table 1:** Distribution network data

The daily load curve of the city is based on measurements of the year 2003. Measurements of real and reactive

power values (P,Q) were performed for each zone z , i.e. for each 150 kV transformer, in time intervals of 15 minutes; hence for a 24-h simulation period $T = \{1\dots96\}$. In order to determine the load at each node in the respective zone, a peak load scenario consisting of one day in 2003 was used to specify the contribution of each node to the peak load of the respective zone. According to this contribution factor, the nodal load is determined as a fraction of the measured load of zone z in time interval T . A load growth of $g = 1\%$ is assumed when investigating years y after 2003. The total system load $L(y)$ is determined according to the cumulated load growth model given by

$$L(y) = L(2003)(1 + g)^{(y-2003)} \quad \forall y \geq 2003 \quad (14)$$

3.1 Integration of PHEV management devices

An agent based approach, relying on utility theory and the game theoretic subclass of strategic form games is chosen for demand management of PHEVs in the power system. Intelligent control devices referred to as PHEV Managers use this approach to distribute, potentially scarce, power efficiently between the connected PHEVs at each power system node or set of nodes [6]. The managers are placed at each power system node n . Based on utility theory, a utility function is assigned to each PHEV. The utility function includes the benefit function

$$B_{v,n}(T, \Omega_{k,n}(T)) = \alpha_{v,n} C_{v,n}^B(\Omega_{v,n}(T)) - \beta_{v,n} C_{v,n}^B(\Omega_{v,n}(T))^2 \quad (15)$$

with

$$\Omega_{v,n}(T) = SOC_{v,n}(T) - SOC_{v,n}^{\min} + \tilde{q}_{v,n} \quad , \quad (16)$$

where $\tilde{q}_{v,n}$ is the acquired energy in per unit of battery capacity $q_{v,n}(T, \theta_{v,n}(T)|\Theta_n(T))$ at time interval T .

The benefit function values the current SOC of the PHEV and is monotonically increasing in SOC and continuously differentiable. The derivative is decreasing in SOC. The variables $\alpha_{v,n}$ and $\beta_{v,n}$ are tuning parameters which affect the recharging behavior. The function is elaborated on in detail in [6]. The utility function consists of benefit function weighted by the parameter $\theta_{v,n}(T)$, which is called agent type, from which the costs of received energy are subtracted. The parameter $\theta_{v,n}(T)$ increases with both, less time and more energy to be recharged. The energy costs are calculated based on an exogenously transmitted energy price signal $\pi_n(T)$. The utility function is defined as

$$u_{v,n}(T, \Omega_{v,n}(T), \theta_{v,n}(T)) = \theta_{v,n}(T) B_{v,n}(T, \Omega_{k,n}(T)) - \pi_n(T) C_{v,n}^B \tilde{q}_{v,n} \quad (17)$$

with

$$\tilde{q}_{v,n} = q_{v,n}(T, \theta_{v,n}(T)|\Theta_n(T)) \quad (18)$$

and

$$q_{v,n}(T, \theta_{v,n}(T)|\Theta_n(T)) = \frac{p_{v,n}(T, \theta_{v,n}(T)|\Theta_n(T))}{\zeta(T) C_{v,n}^B} \quad , \quad (19)$$

where $1/\zeta(T)$ is the hourly fraction of the time interval length, here chosen to be 15 minutes; hence in this case $\zeta(T) = 4$. The variable $p_{v,n}(T, \theta_{v,n}(T)|\Theta_n(T))$ denotes

the power assigned to PHEV v in time interval T . Consequently, $q_{v,n}(T, \theta_{v,n}(T)|\Theta_n(T))$ gives the assigned energy rated in per unit of battery capacity. Both are dependent on $\Theta_n(T)$ which is the distribution of the agent types $\theta_{v,n}(T)$ at node n .

The PHEV Managers maximize the sum of the utility functions of the PHEVs connected at node n , ensuring that the battery of the individual PHEV is not overloaded, that the power constraint of the PHEV and that of the respective node, i.e. the rating of the 11/22 kV transformer, are not violated. The exogenous electricity price signal $\pi_n(T)$, which is used as input for the optimization at the nodes, is assumed to be constant over the day. Hence, at the optimization start, $\pi_n(T) = \pi(T)$, $\forall n \in \mathcal{N}$. The managers use a receding horizon, multi period optimization in order to take vehicle arrival and load forecasts into account. The number of time intervals considered for the receding horizon optimization is given by ΔT_n^{MPC} . For shortness, in this paper it is assumed that $\Delta T_n^{\text{MPC}} = 0$. Each PHEV Manager maximizes

$$\sum_{t=T}^{T+\Delta T_n^{\text{MPC}}} \sum_{v=1}^{N_n^{\text{PHEV}}(t)} u_{v,n}(\Omega_{v,n}(t), \theta_{v,n}(t)) \quad (20)$$

subject to

$$p_{v,n}^{\min}(t) \leq p_{v,n}(t, \theta_{v,n}(t)|\Theta_n(t)) \leq p_{v,n}^{\max}(t) \quad (a)$$

$$SOC_{v,n}^{\min} \leq SOC_{v,n}(t) + \sum_{t=T}^{T+\Delta T_n^{\text{MPC}}} q_{v,n}(\cdot) \leq SOC_{v,n}^{\max} \quad (b)$$

$$P_n^{\min}(t) \leq \sum_{v=1}^{N_n^{\text{PHEV}}(t)} p_{v,n}(t, \theta_{v,n}(t)|\Theta_n(t)) \leq P_n^{\max}(t) \quad (c) \quad \forall n \in \mathcal{N}$$

with

$$\alpha_{v,n} = \pi^{\max} = \frac{\pi_{\text{gasoline}}}{\rho_{\text{gasoline}} \eta_{\text{ICE}}} \eta_{\text{mot}} \eta_c \eta_{dc} \quad (21)$$

$$\beta_{v,n} = \frac{\pi^{\min} - \alpha_{v,n}}{-2} \quad ,$$

where (20)(a) holds the power setpoint of vehicle v between the maximum connection rating for charging, denoted $p_{v,n}^{\max}(t)$ and the minimum connection rating for discharging, denoted $p_{v,n}^{\min}(t)$, in a V2G case, which can also be captured by this formulation. Here, $p_{v,n}^{\min}(t)$ is set to zero. Constraint (20)(b) ensures that the SOC does not exceed $SOC_{v,n}^{\max}$ which denotes the desired SOC at departure and (20)(c) ensures that the 11/22 kV transformer is not overloaded. The parameter $\alpha_{v,n}$ is determined by the gasoline price and is weighted by the converter efficiencies in the powertrain. The parameter $\beta_{v,n}$ is determined by the assumed, constant electricity price signal during the day, thus $\pi^{\min} = \pi_n(T)$. Note that in case of congestion at the node n the price signal is endogenously determined and mutated by the PHEV Manager. This results in the desired PHEV charging behavior.

3.2 Integration of supervisory PHEV management devices

The PHEV Managers ensure that the transformers at the lowest voltage levels are not overloaded. However, due to the wide scale utilization of PHEVs, the load in one zone or several zones may be massively increased so that the transformers at higher voltage levels are overloaded. In order to avoid the overloading of assets on higher network

levels, a Supervisory PHEV Manager (S-PHEV Manager) is integrated on the level of the 150 kV-11/22 kV transformers. The concept is illustrated in Fig. 4(a). The S-PHEV Manager controls the demand of power which may be distributed by the PHEV Managers active on the lower voltage levels of zone z and ensures that the 150 kV-11/22 kV transformer is not overloaded.

The S-PHEV Manager performs an optimization similar to the one of the PHEV Manager. The S-PHEV Manager clusters the PHEVs controlled by the PHEV Managers in the supervised zone. Subsequently it uses the power setpoints $\hat{p}_{v,n}(T)$, determined by the PHEV Managers, as the upper bound of its individual vehicle power consumption constraint. For a V2G case, the lower bound would be exchanged. The S-PHEV Manager thus maximizes

$$\sum_{n=1}^{N_z} \sum_{v=1}^{N_n^{\text{PHEV}}(T)} u_{v,n} \left(\Omega_{v,n}(T), \theta_{v,n}(T) \right) \quad (22)$$

subject to

$$p_{v,n}^{\min}(T) \leq p_{v,n}(T, \theta_{v,n}(T) | \Theta_n(T)) \leq \hat{p}_{v,n}(T) \quad (a)$$

$$SOC_{v,n}^{\min} \leq SOC_{v,n}(T) \leq SOC_{v,n}^{\max} \quad (b)$$

$$P_z^{\text{Tr},\min}(T) \leq \sum_{n=1}^{N_z} \sum_{v=1}^{N_n^{\text{PHEV}}(T)} p_{v,n}(\cdot) \leq P_z^{\text{Tr},\max}(T) \quad (c)$$

where the variable $P_z^{\text{Tr},\max}(T)$ gives the maximum load of zone z which can be supplied by the 150 kV transformer in time interval T and $P_z^{\text{Tr},\min}(T)$ gives the minimum load of this transformer in a possible V2G case; here $P_z^{\text{Tr},\min}(T)$ is set to zero.

Besides transformer overloading at the 150 kV level, excessive PHEV demand can cause violations of voltage bands on the 11/22 kV level. Changing the tap position of the tap changing transformers can mitigate voltage problems in the zones. Should the tap variations result in voltages not compliant with the 11/22 kV level boundaries, the S-PHEV Manager needs to decrease the PHEV load for the particular zone during this time step and shift the load to later time intervals. In order to find the maximum load which can be supplied to the PHEV fleet in a zone, the concept of voltage stability margins can be used [10]. The zone, depicted in Fig. 4(a), and its voltage dependence, i.e. the complex voltage \underline{U}_z at the busbar and the total load of the connected nodes, can be modeled using the Thevenin-Equivalent, as illustrated in Fig. 4(b). The parameters of the Thevenin equivalent, i.e. $\underline{E}_{\text{th}}$, R_{th} and X_{th} , can be found by solving

$$\begin{bmatrix} \Re(\underline{U}_{z,1}) & \Im(\underline{U}_{z,1}) & -P_{z,1} & -Q_{z,1} \\ -\Im(\underline{U}_{z,1}) & \Re(\underline{U}_{z,1}) & Q_{z,1} & -P_{z,1} \\ \Re(\underline{U}_{z,2}) & \Im(\underline{U}_{z,2}) & -P_{z,2} & -Q_{z,2} \\ -\Im(\underline{U}_{z,2}) & \Re(\underline{U}_{z,2}) & Q_{z,2} & -P_{z,2} \end{bmatrix} \cdot \begin{bmatrix} \Re(\underline{E}_{\text{th}}) \\ \Im(\underline{E}_{\text{th}}) \\ R_{\text{th}} \\ X_{\text{th}} \end{bmatrix} = \begin{bmatrix} \Re(\underline{U}_{z,1}^2) + \Im(\underline{U}_{z,1}) \\ 0 \\ \Re(\underline{U}_{z,2}^2) + \Im(\underline{U}_{z,2}) \\ 0 \end{bmatrix} \quad (23)$$

where $P_{z,1}$, $Q_{z,1}$ and $P_{z,2}$, $Q_{z,2}$ denote the active and reactive power consumption of zone z for two load cases while $\Re(\cdot)$ and $\Im(\cdot)$ give the real and imaginary parts of their argument, respectively. The chosen cases incorporate

a situation at nominal, 100%, PHEV load and one where PHEV load is at 90 % in the respective zone.

Having found the parameters of the Thevenin equivalent, the relation

$$\underline{U}_z^4 + (2P_z R_{\text{th}} + 2Q_z X_{\text{th}} - \underline{E}_{\text{th}}^2) \underline{U}_z^2 + (P_z^2 + Q_z^2)(R_{\text{th}}^2 + X_{\text{th}}^2) = 0 \quad (24)$$

can be derived from the Thevenin-circuit. Setting the \underline{U}_z to the minimal acceptable voltage for the zone and adding a markup for the lowest nodal voltage within the zone, one can derive a maximum allowable active power $P_z^{\text{V,max}}$. This active power can be supplied to the PHEV fleet in zone z without causing violations of the lower voltage bound, thus ensuring power quality in the respective city region. This maximum active power derived from the voltage relation is denoted $P_z^{\text{V,max}}$ and is subsequently used as the upper bound in constraint (22)(c) of the S-PHEV Manager.

The complete algorithm which is used for managing the PHEV demand in Zurich's electricity network is illustrated and described in Fig. 5 on page 5.

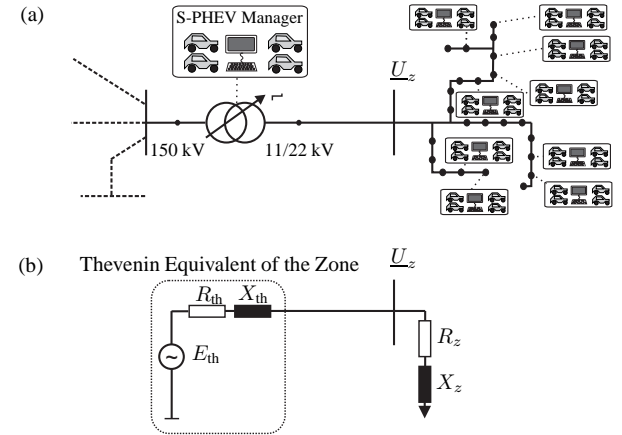


Figure 4: (a) Zone fed by a 150 kV-11/22 kV tap changing transformer. A Supervisory PHEV Manager (S-PHEV Manager) controls the underlying PHEV Managers while the PHEV Managers at each node control the PHEVs connected to the 11/22 kV-400 V transformer. (b) Thevenin equivalent of the zone in Fig. 4(a) and its load. It is used to determine the maximal total load of all underlying PHEV Managers which ensures compliance with voltage stability limits

4 CASE STUDIES OF PHEV IMPACT ON ZURICH'S ELECTRICITY SYSTEM

MATSim is used to simulate a transportation example of Switzerland comprised of ca. 850'000 PHEVs, each with a battery capacity of 10 kWh. The transportation simulation incorporates the cars belonging to the population of city of Zurich as well as those of commuters. Fig. 6 illustrates the evolution of PHEVs connected in the metropolitan area of Zurich. During night time ca. 170'000 PHEVs are parked in the city of Zurich. During day time the number of PHEVs parked reaches ca. 230'000 at 14:00. This rise in the number of PHEVs can be explained by working hours as well as shopping opportunities in Zurich. The small dip in the number of connected PHEVs occurring around noon can be explained by agents departing in order to go shopping or for lunch. The number of connected agents decreases in the evening as agents which represent commuters which quit their activities and leave the city.

around 16.5 Mio CHF for the replacement of the eleven 150 kV transformers which are overloaded at peak load time. Fourteen cables are overloaded in the *uncontrolled* 2010 scenario. Due to space constraints both results are not depicted.

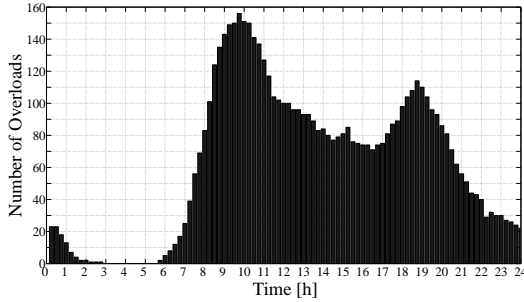


Figure 9: Number of overloaded 11/22 kV transformer stations in 2010 caused by *uncontrolled* PHEV recharging

4.2 Comparison of Uncontrolled and Controlled Charging of Electric Vehicles in 2010 and 2030

In order to ensure a secure network operation without overloads and voltage violations the hierarchical control method described in the preceding sections has been utilized for both the year 2010 and the year 2030.

Fig. 10 shows the nodal control price signals $\pi_n(T)$ which are endogenously determined by the hierarchical control structure in case of network congestion. The base load of the year 2010 is used. The signals are distributed to the PHEVs, which adapt their recharging behavior according to the hierarchical control structure and their individual utility function. A large number of control signal peaks appears for the current system expansion state, especially during the midday and evening hours. Less peaks can be seen in the morning hours. This is due to the lower conventional system loading, i.e. non-vehicular load. It should be noted that the value of the control price signal at a node encodes the power system and the vehicle fleet state in the respective time interval. The higher the control price signal, the larger the connected fleet and/or their energy requirement. The latter is determined by the utility function and the temporally variable individual agent parameter $\theta_{v,n}(T)$.

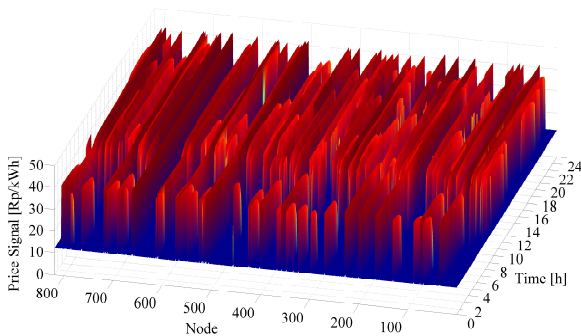


Figure 10: Endogenously determined nodal control price signals $\pi_n(T)$ of all PHEV Managers operated in Zurich

The demand management scheme avoids transformer overloads on the 11/22 kV and on the 150 kV level. The scheme would allow postponing grid expansion investments due to electric mobility by better utilization of already installed assets, as PHEV load is shifted to low-

demand times where enough capacity is available.

Fig. 11 depicts the load curves used for the year 2010 and 2030 for the base cases and with additional PHEV charging in controlled and uncontrolled manner. The solid and dashed lines illustrate load curves for *controlled* and *uncontrolled* PHEV recharging scenarios, respectively. The system peak load is, compared to the *uncontrolled* scenario, reduced by the implementation of *controlled* recharging. Excessive PHEV load is shifted to later times if possible. This shifting effect has a minor impact on the load curves in both years because the network is heavily stressed. Even taking advantage of the vehicles temporal flexibility in being recharged does not to recharge all of them accordingly. Many PHEVs have to depart with energy levels less than their desired SOC.

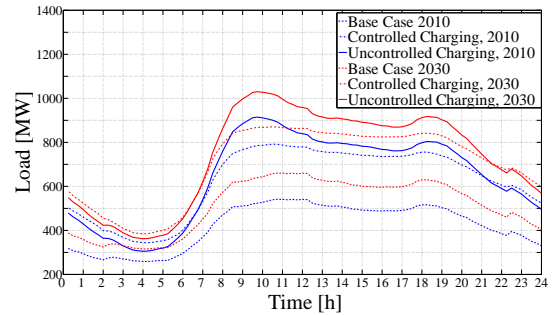


Figure 11: Zurich system load with uncontrolled and controlled PHEV recharging

The shape of the base load in 2030, depicted by the red dotted line in Fig. 11, has the same shape as that in 2010, albeit with a higher peak load of about 700 MW. For this case, most of the network infrastructure is left unchanged. Only the 11/22 kV transformer ratings are fitted to the load data as explained before. This situation poses a worst case scenario for the wide scale utilization of electric mobility because many network assets are more heavily loaded than before. The system peak load is increased to almost 1100 MW in the *uncontrolled* case. However, with *controlled* PHEV load, the load curve is flattened, especially during the morning hours. Similarly to 2010, the 2030 load curve exhibits an almost flat plateau between 09:00 and 13:00.

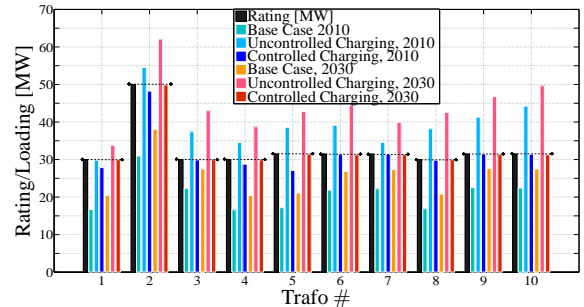


Figure 12: Rating and loading of selected 150 kV transformers in 2010 (blue group) and 2030 (red group) for the base load cases and PHEV charging scenarios

Fig. 12 shows the loading of selected transformers on the 150 kV level at 09:30 for both charging cases and for the base case in both 2010 (blue bar group) and 2030 (red bar group). The maximum permissible loading of each transformer is indicated by the black bars, and by the dashed, black, horizontal lines.

In general, the loading of the depicted transformers is substantially increased by the PHEVs. Ten overloads can

be seen at 09:30 for the *uncontrolled* charging scenario of 2010. In the *controlled* charging scenario, six transformers are loaded to their maximum rating. This is due to the load being capped by their maximum rating. For the other four transformers do not reach their maximum rating as the underlying 11/22 kV transformers limit the total load of these zones. In summary, the load at the individual transformers is equal to or lower than in the *uncontrolled* scenario.

In 2030, where the base load is substantially higher, the *uncontrolled* charging of PHEVs overloads all depicted transformers. These overloads are fully mitigated by the hierarchical control scheme presented before. The control scheme avoids the overloading by shifting the PHEV load away to later times while maximally loading the transformers to their allowed rating.

5 CONCLUSIONS

This paper shows how power systems and transportation systems can be combined in order to effectively assess the impact of wide scale electric mobility on the distribution system of a municipality, to delineate expansion needs introduced by electric mobility.

In contrast to the simplified models of power systems, transport behavior and charging characteristics often used in current literature, the presented work uses a detailed modeling approach, both for power and transportation systems, to gain additional information. By detailed simulation of agent behavior, the step from qualitative to realistic quantitative results can be made.

The detailed knowledge of temporal and spatial recharging behavior allows investigation of the impact of uncontrolled charging on the electricity network of a large metropolitan area. The utilized electricity network consists of multiple voltage levels and spatially, as well as temporally, varying load data.

It is found that uncontrolled recharging, even with today's relatively strong electricity network, leads to overloads on multiple voltage levels. Uncontrolled charging increases the overall system peak load and changes the system load curve.

In addition, the paper presents a predictive, distributed, hierarchical demand management scheme which considers transformer loading and voltage stability limits on different levels and is able to mitigate the hazards caused by uncontrolled recharging. The control scheme fully takes advantage of the flexibility of the PHEV load while avoiding unanticipated, undesirable PHEV recharging behavior. The application of the control scheme demonstrates that violation of transformer loading and voltage stability limits can be avoided, shifting excessive PHEV demand to later times while still recharging the PHEVs to their desired energy level.

Finally, the application of the control scheme in the large electricity network demonstrates that effective control schemes can be fully integrated into the current power system. The presented control method allows the postponement of substantial investments in electricity distribution assets which would be caused by electric mobility while utilizing the installed assets more efficiently.

6 ACKNOWLEDGEMENTS

The work is sponsored by the Swiss Federal Institute of Technology (ETH) Zurich under research grant TH 2207-3, by the Swiss Federal Office of Energy, ETH Zurich and by the municipal utility company of Zurich, *ewz*. The authors would like to thank Turhan Demiray for integrating MATLAB[®] and NEPLAN[®] and Emil Igglund for proof reading the paper.

REFERENCES

- [1] M.D. Galus, M. Zima, and G. Andersson. On integration of PHEVs into existing power system structures. *Energy Policy*, 38:6736–6745, 2010.
- [2] J.A. Pecas Lopes, F.J. Soares, and P.M. Rocha Almeida. Identifying management procedures to deal with connection of electric vehicles in the grid. In *Proceedings of IEEE PowerTech*, Bucharest, Romania, 2009.
- [3] P. Mohseni and R. G. Stevie. Electric vehicles: holy grail or fool's gold. In *Proceedings of IEEE General Meeting*, Minneapolis, MN, USA, 2010.
- [4] K. Clement-Nyns, E. Haesen, and J. Driesen. The impact of charging plug-in hybrid electric vehicles on a residential distribution grid. *IEEE Transactions on Power Systems*, 25(1):371–380, 2010.
- [5] M. D. Galus and G. Andersson. Power System Considerations of Plug-In Hybrid Electric Vehicles based on a Multi Energy Carrier Model. In *Proceedings of IEEE Power and Energy Society (PES) General Meeting*, Calgary, Canada, 2009.
- [6] M. D. Galus and G. Andersson. Demand management for grid connected Plug-In Hybrid Electric Vehicles (PHEV). In *Proceedings of IEEE Energy 2030*, Atlanta, GA, USA, 2008.
- [7] M. Balmer, K. W. Axhausen, and K. Nagel. Agent-based demand-modelling framework for large-scale microsimulations. *Transportation Research Record: Journal of the Transportation Research Board*, 1985(2006):125–134, 2006.
- [8] D. Charypar and K. Nagel. Generating complete all-day activity plans with genetic algorithms. *Transportation*, 32(4):369–397, 2005.
- [9] R. Waraich, M.D. Galus, C. Dobler, M. Balmer, G. Andersson, and K.W. Axhausen. Plug-In Hybrid Electric Vehicles and Smart Grid: Investigations based on a Micro-Simulation. In *Proceedings of the Conference of the International Association for Travel Behaviour Research (IABTR)*, Jaipur, India, 2009.
- [10] M. H. Haque. On-line monitoring of maximum permissible loading of a power system within voltage stability limits. *IEE Proceedings on Generation, Transmission and Distribution*, 150(1):107–112, 2003. 1350-2360.